# The projective linear transition map for constructing smooth surfaces

## Abstract

We exhibit the essentially unique projective linear (rational linear) reparameterization for constructing $C^s$ surfaces of genus $g > 0$, from tensor-product splines. Conversely, for quadrilaterals and isolated vertices of valence 8, we show constructively for $s = 1, 2$ that this map yields a projective linear spline space for surfaces of genus greater or equal to 1. This establishes the reparametrization to be the simplest possible transition map.

## Keywords

reparameterization, unique rational linear transition map, free-form spline surface, quad meshes, topology, non-zero genus, $G^s$ geometric continuity

## 1. INTRODUCTION

The Euler formula[1] (Euler-Poincaré characteristic) allows for closed polyhedra of topological genus $g > 0$ consisting of an arrangement of quadrilaterals that is a rectangular grid except for $-\chi = 2g - 2$ isolated vertices of valence 8.[2] Figure 1 shows an example of genus $g = 2$, with two isolated vertices of valence 8 (on the front and back of the waist-line of a figure-8 double torus) and Figure 6 shows examples of higher genus.

Using Ricci flow, Gu and co-workers have generated re-approximations of triangulations by quadrilateral meshes with $-\chi$ vertices of valence 8 (see [GHJ$^+$08] for an illustration of their pipeline[3]). Moreover, these quad-meshes can be angle-preserving images of subsets of the Euclidean plane whose boundaries have been suitably identified. We may therefore interpret them as conformal parameterizations of triangulated data in $\mathbb{R}^3$.

A natural generalization to smooth, $s$ times differentiable, conformally parameterized surfaces, is to associate a tensor-product spline with each quadrilateral. However, the 8-valent points interrupt the rectangular grid connectivity required by tensor-product splines. According to [GHJ$^+$08] they represent 'topological obstructions' where smooth surfaces are 'difficult to construct, unstable, and error-prone'. By Euler's count we cannot hope to eliminate the 8-valent vertices. And, by a result of Milnor [Mil58], we cannot hope to use just linear changes of the parameters to transition between the tensor-product spline pieces of a regularly parameterized smooth closed surfaces of genus $g > 1$ in $\mathbb{R}^3$, i.e. we cannot hope for an affine atlas. (For genus $g = 1$, the construction of an affine atlas is trivial, since the torus is just a tensor-product grid with opposing edges identified.)

The next simplest alternative to an affine atlas, compatible with conformal parameterizations, is a fractional linear atlas. In differential geometry, linear fractional transformations are usually associated with the class of *Moebius transformations*: $\boldsymbol{\mu}(z) := \frac{az+b}{cz+d} : \mathbb{C} \to \mathbb{C}$ where $a, b, c, d \in \mathbb{C}$ and $ad - bc = 1$. Moebius transformations are bijective conformal orientation-preserving maps. They suffice to build a complex fractional linear atlas when proving the Uniformization Theorem (which yields a classification of surfaces according to curvature [wik09]).

---

[1]$v - e + f = \chi$ where $v, e, f$ are respectively the numbers of vertices, edges and faces in a given polyhedron and $\chi = 2 - 2g$ is the Euler characteristic

[2]To see this, observe that we can exclusively associate with each 4-valent vertex four half-edges and four quarters of attached quads so that its net contribution to the Euler count is $1 - 4/2 + 4/4 = 0$. For each 8-valent vertex the contribution is $1 - 8/2 + 8/4 = -1$.

[3][GHJ$^+$08] also proposes decreasing the number of singularities. This is is not important in the present paper.
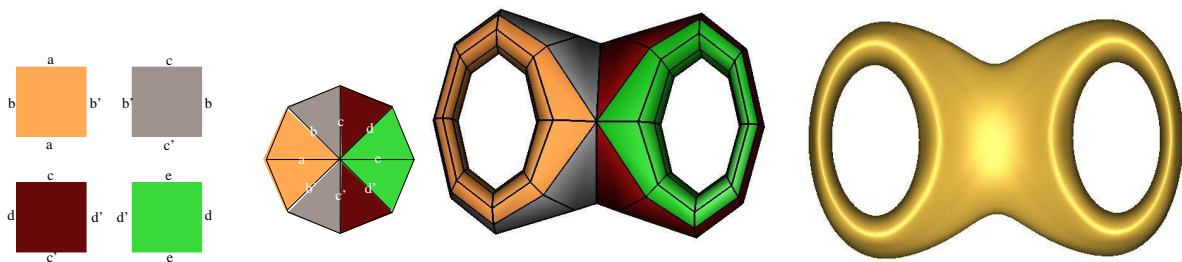


Fig. 1. Figure-8: *left*: Identification of edges of the 4 quadrilaterals. *middle*: Embedding in $\mathbb{R}^3$ with $2g - 2 = 2$ corner points of valence 8. *right*: Corresponding smooth spline surface with central saddle shape.

By contrast, the focus of the present paper is on real rational linear maps $\rho$ of the type

$$\rho(u,v) := \begin{bmatrix} \rho^{[1]} \\ \rho^{[2]} \end{bmatrix} := \begin{bmatrix} \frac{a_1+b_1u+c_1v}{d_1+e_1u+f_1v} \\ \frac{a_2+b_2u+c_2v}{d_2+e_2u+f_2v} \end{bmatrix}, \tag{1}$$

where $a_i, b_i, \ldots, f_i$ are real scalars. The reason for this choice becomes apparent when using the Moebius map $\boldsymbol{\mu}$, respectively the rational linear map $\rho$ as reparameterization $r : \mathbb{R}^2 \to \mathbb{R}^2$ so that two surface pieces $\mathbf{p}$ and $\mathbf{q}$, sharing an edge parameterized by $t$, have identical derivatives across the edge up to order $s$:

$$\partial^i \mathbf{p}(t,0) = \partial^i(\mathbf{q} \circ r)(t,0), \quad i = 0, \ldots, s. \tag{2}$$

When using $r = \boldsymbol{\mu}$ in this way, the basic requirement for adjusting the orientation of counterclockwise arranged patches, $\boldsymbol{\mu}(t,0) = (0,t)$, fixes $\boldsymbol{\mu}(u,v) = -v + u\sqrt{-1}$ and hence accommodates exclusively 4 patches joining, not 8. This is because the group of Moebius transformations, the projective, special linear group over the complex numbers, $PSL(2,\mathbb{C})$, endows $\boldsymbol{\mu}$ with only 6 real degrees of freedom. By contrast, $\rho$ is chosen from the 8-dimensional group $SL(3,\mathbb{R})$ which, as we will show, can accommodate constructions with 8-valent vertices. Nevertheless, $\rho$ is in some sense *the simplest map*: expressed as a real rational map, $\boldsymbol{\mu}$ is of degree 2 over 2, while $\rho$ is of degree 1 over 1.

**Overview.** In Section 2, we collect the constraints that (2) imposes on $\rho$. In Section 3, these constraints are then applied to set the free parameters of $\rho$. Somewhat surprisingly, we find that there is an essentially unique map $\rho$ that can potentially serve as reparameterization. In Section 4, we show that $\rho$ indeed enables connecting tensor-product splines given a quadrilateral control net with isolated vertices of valence 8 and valence 4 everywhere else. We outline algorithms for the construction of $C^1$ and $C^2$ surfaces satisfying the $G^1$, respectively $G^2$ constraints (2) and using one spline patch per quad. Our aim here is to show existence of a reasonable construction not necessarily exhibit a best.

**Background.** We follow the constructive approach to surfaces used in geometric modeling rather than the analytic approach via charts of differential geometry which assumes the existence of a surface: our spline patches and reparameterizations are defined on finite, *closed* sets, namely the unit square, denoted $\square \subseteq \mathbb{R}^2$. And we join abutting patches rather than overlapping charts. One can, of course, obtain an atlas from the patch-based construction as shown, e.g., in [Pet02].

Since our focus is the rational linear reparameterization $\rho$, we intentionally do not survey here the rich literature on *general* surface constructions. For the reader interested in such constructions, the introduction of Karciauskas and Peters [KP09] gives an overview of recent $C^2$ constructions with general connectivity. For an example of a construction via charts, see e.g. Ying and Zorin [YZ04] and for a polynomial construction with general connectivity, see e.g.. Loop and Schaefer [LS08]. The relevant observation for the present paper is that by [PF09, Lemma 4], *all these general constructions must employ quadratic or higher-degree reparameterizations* (see also Section IV below). We cannot, therefore, point to the literature to find constructions based on $\rho$.

## 2. Constraints on the transition map for $G^2$ continuity

We are looking to determine a rational linear reparameterization

$$\rho : \square \subsetneq \mathbb{R}^2 \to \mathbb{R}^2 \tag{3}$$

where $\square$ is the unit square. The reparameterization is to allow two tensor-product patches $\mathbf{p} : \square \subsetneq \mathbb{R}^2 \to \mathbb{R}^d$ and $\mathbf{q} : \square \subsetneq \mathbb{R}^2 \to \mathbb{R}^d$ to join smoothly across the common boundary

$$\mathbf{q}(t,0) = \mathbf{p}(0,t). \tag{4}$$

Equation (4) implies

$$\rho(t,0) = (0,t) \tag{5}$$

and therefore

$$\partial_1^k \rho^{[1]}(t,0) = 0, \; \partial_1^1 \rho^{[2]}(t,0) = 1 \text{ and } \partial_1^k \rho^{[2]}(t,0) = 0 \text{ for } k > 1. \tag{6}$$

### 2.1 $G^1$ constraints

The reparameterization to be determined is used in the $G^1$ constraints

$$(\partial_2 \mathbf{q})(t,0) = (\partial_2(\mathbf{p} \circ \rho))(t,0)$$
$$= (\partial_1 \mathbf{p} \circ \rho)\partial_2 \rho^{[1]}(t,0) + (\partial_2 \mathbf{p} \circ \rho)\partial_2 \rho^{[2]}(t,0). \tag{7}$$

We want the $G^1$ constraints to be unbiased, i.e. structurally symmetric as we exchange $\mathbf{p}$ with $\mathbf{q}$. Therefore

$$(\partial_2 \rho^{[1]})(t,0) = -1. \tag{8}$$

Also, when $n$ patches join $\rho^{[2]}$ must satisfy

$$\tau := \partial_2\rho^{[2]}(0,0) = 2\cos\frac{2\pi}{n}. \tag{9}$$

This yields the unbiased $G^1$ constraints

$$(\partial_2\mathbf{q})(t,0) + (\partial_1\mathbf{p}\circ\rho)(t,0) = (\partial_2\mathbf{p}\circ\rho)\partial_2\rho^{[2]}(t,0), \tag{7'}$$

$$\text{and, at } (u,v)=(0,0), \quad \partial_2\mathbf{q} + \partial_1\mathbf{p} = \tau\partial_2\mathbf{p}. \tag{10}$$

If we differentiate (7') along the boundary, i.e. differentiate with respect to $t$, then by (6)

$$(\partial_1\partial_2\mathbf{q})(t,0) + (\partial_2\partial_1\mathbf{p})(0,t)$$
$$= (\partial_2^2\mathbf{p})(0,t)(\partial_2\rho^{[2]})(t,0) + (\partial_2\mathbf{p})(0,t)(\partial_1\partial_2\rho^{[2]})(t,0) \tag{11}$$

$$\text{and, at } (u,v)=(0,0), \quad \partial_1\partial_2\mathbf{q} + \partial_2\partial_1\mathbf{p} = \tau\partial_2^2\mathbf{p} + \partial_2\mathbf{p}\partial_1\partial_2\rho^{[2]}. \tag{12}$$

## 2.2 $G^2$ constraints

The reparameterization to be determined defines the $G^2$ constraints

$$(\partial_2^2\mathbf{q})(t,0) = (\partial_2^2(\mathbf{p}\circ\rho))(t,0) \tag{13}$$
$$= (\partial_1^2\mathbf{p})(0,t) - 2(\partial_1\partial_2\mathbf{p})(0,t)\partial_2\rho^{[2]}(t,0) + (\partial_2^2\mathbf{p})(0,t)(\partial_2\rho^{[2]})^2(t,0)$$
$$+ (\partial_1\mathbf{p})(0,t)(\partial_2^2\rho^{[1]})(t,0) + (\partial_2\mathbf{p})(0,t)(\partial_2^2\rho^{[2]})(t,0).$$

In particular, at $(u,v)=(0,0)$:

$$\partial_2^2\mathbf{q} = \partial_1^2\mathbf{p} - 2\partial_1\partial_2\mathbf{p}\tau + 2\partial_2^2\mathbf{p} + \partial_1\mathbf{p}\partial_2^2\rho^{[1]} + \partial_2\mathbf{p}\partial_2^2\rho^{[2]}. \tag{14}$$

Substituting (12) and (10), we symmetrize the $G^2$ constraint at $(u,v)=(0,0)$

$$\partial_2^2\mathbf{q} - \partial_2\partial_1\mathbf{q}\tau \overset{(12)}{=} \partial_1^2\mathbf{p} - \partial_1\partial_2\mathbf{p}\tau + \partial_1\mathbf{p}\partial_2^2\rho^{[1]}$$
$$+ \partial_2\mathbf{p}(-\tau\partial_1\partial_2\rho^{[2]} + \partial_2^2\rho^{[2]}),$$

$$\partial_2^2\mathbf{q} - \partial_2\partial_1\mathbf{q}\tau + \frac{1}{2}\partial_2\mathbf{q}\partial_2^2\rho^{[1]} \overset{(10)}{=} \partial_1^2\mathbf{p} - \partial_1\partial_2\mathbf{p}\tau + \frac{1}{2}\partial_1\mathbf{p}\partial_2^2\rho^{[1]}$$
$$+ \partial_2\mathbf{p}\left(-\tau\partial_1\partial_2\rho^{[2]} + \partial_2^2\rho^{[2]} + \frac{\tau}{2}\partial_2^2\rho^{[1]}\right). \tag{15}$$

For $\mathbf{t} := \partial_2\mathbf{p}(0,0) = \partial_1\mathbf{q}(0,0)$, an unbiased construction at $(u,v) = (0,0)$ implies $\mathbf{t} \cdot (\partial_2^2\mathbf{q} - \partial_2\partial_1\mathbf{q}\tau + \frac{1}{2}\partial_2\mathbf{q}\partial_2^2\rho^{[1]}) = \mathbf{t} \cdot (\partial_1^2\mathbf{p} - \partial_1\partial_2\mathbf{p}\tau + \frac{1}{2}\partial_1\mathbf{p}\partial_2^2\rho^{[1]})$ and, since we rule out singular constructions, $\mathbf{t} \cdot \mathbf{t} \neq 0$ so that, at $u = v = 0$,

$$\tau\partial_1\partial_2\rho^{[2]} - \partial_2^2\rho^{[2]} = \frac{\tau}{2}\partial_2^2\rho^{[1]} \tag{16}$$

must hold.

## 3. THE PROJECTIVE LINEAR TRANSITION MAP

We note that the previous section did not make any assumption on the surface pieces $\mathbf{p}$ and $\mathbf{q}$ or the map $\rho$ other than that they be sufficiently smooth. Neither valence, nor polynomiality, nor the number of boundary edges of the surface pieces mattered.

Remarkably, in this very general setting, the projective linear reparameterization is essentially unique.

*Theorem 1:* The transition map $\rho : \mathbb{R}^2 \to \mathbb{R}^2$ of (1) for the $G^2$ construction of a $C^2$ surface is unique up to the values of $\tau := \partial_2\rho^{[2]}(0,0)$ and $\sigma := \partial_2\rho^{[2]}(1,0)$:

$$\rho(u,v) := \frac{1}{1+v(\tau-\sigma)}\begin{bmatrix} -v \\ u+\tau v \end{bmatrix}. \tag{1'''}$$

*Proof:* By (5), $\rho(t,0) = (0,t)$, we have

$$\rho^{[1]} : \frac{a_1 + b_1 t}{d_1 + e_1 t} = 0 \implies a_1 = b_1 = 0 \tag{17}$$

$$\rho^{[2]} : \frac{a_2 + b_2 t}{d_2 + e_2 t} = t \implies a_2 = e_2 = 0, b_2 = d_2. \tag{18}$$

Therefore $\rho$ simplifies to

$$\rho(u,v) := \begin{bmatrix} \frac{c_1 v}{d_1 + e_1 u + f_1 v} \\ \frac{d_2 u + c_2 v}{d_2 + f_2 v} \end{bmatrix}. \tag{1'}$$

Next (8) implies

$$-1 = \partial_2 \rho^{[1]}(t,0) = \frac{c_1}{d_1 + e_1 t} \implies e_1 = 0, d_1 = -c_1. \tag{19}$$

On the other hand, $\partial_2 \rho^{[2]}(t,0) = \frac{c_2}{d_2} - t\frac{f_2}{d_2}$ and (9) implies

$$\partial_2 \rho^{[2]}(0,0) = \frac{c_2}{d_2} = \tau. \tag{20}$$

Therefore

$$\rho(u,v) := \begin{bmatrix} \frac{-d_1 v}{d_1 + f_1 v} \\ \frac{u + \tau v}{1 + v f_2/d_2} \end{bmatrix}. \tag{1''}$$

If we define $\sigma := \partial_2 \rho^{[2]}(1,0) = \tau - \frac{f_2}{d_2}$ then $\rho^{[2]}(u,v) = \frac{u+\tau v}{1+v(\tau-\sigma)}$ and we can abbreviate

$$\alpha(t) := \partial_2 \rho^{[2]}(t,0) = \tau(1-t) + \sigma t, \tag{21}$$
$$\partial_2^2 \rho^{[2]}(t,0) = -2(\tau-\sigma)\alpha(t). \tag{22}$$

Next, we observe that $\partial_2^2 \rho^{[1]}(t,0) = -\frac{2f_1}{c_1} = \partial_2^2 \rho^{[1]}(0,0)$. Therefore (16) implies

$$\partial_2^2 \rho^{[1]} = -\frac{2f_1}{c_1} = \frac{2}{\tau}(\tau \partial_1 \partial_2 \rho^{[2]} - \partial_2^2 \rho^{[2]}) = 2(\sigma - \tau) + 4(\tau - \sigma) \tag{23}$$
$$= 2(\tau - \sigma).$$

All together, this yields (1'''). ∎

We note that by (19) and (23) both $\partial_2 \rho^{[1]}(t,0)$ and $\partial_2^2 \rho^{[1]}(t,0)$ are constant functions and by (21) and (22) both $\partial_2 \rho^{[2]}(t,0)$ and $\partial_2^2 \rho^{[2]}(t,0)$ are linear functions and that the inverse of $\rho$ is also rational linear:

$$\rho^{-1}(s,t) := \frac{1}{1 + s(\tau - \sigma)}\begin{bmatrix} t + s\tau \\ -s \end{bmatrix}. \tag{24}$$
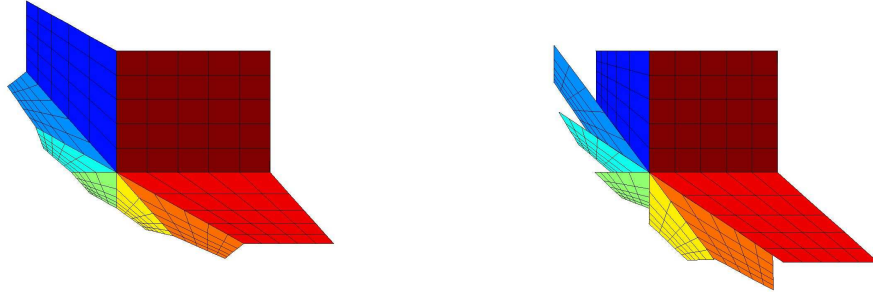


Fig. 2. Illustration of Lemmas 1 and 2. Eight-fold composition of $\rho$ with itself with (*left*) all $\sigma_k$ equal, (*right*) $\sigma_k := \tau\frac{m(k)-2}{m(k)}$ where $m := [2,8,6,8,2,8,6,8]$. The *brown* square $\square$ in the upper right quadrant is mapped first to $\rho(\square)$ (*blue*, upper left quadrant), then in counterclockwise order to $\rho \circ \rho(\square)$ (*medium blue*), etc. to arrive back at $\rho^8(\square) = \rho \circ \ldots \circ \rho = \square$.

Next we check for all reasonable $n$ by symbolic substitution that our rational linear map satisfies the *composition constraint* [Hah89] up to any order of differentiation. That is, $n$-fold composition of $\rho$ with itself yields the identity and the images wind around the origin exactly once without overlap; see Figure 2 for $n = 8$.

*Lemma 1:* For $n = 3, \ldots, 24$, for $\sigma_k := \partial_2 \rho_k^{[2]}(1,0)$ all equal and $\tau := \partial_2 \rho^{[2]}(0,0) = 2\cos\frac{2\pi}{n}$, the $n$-fold composition $\rho^n = \rho \circ \ldots \circ \rho = \text{id}$, i.e. $\rho^n$ is the identity; and $\rho^i(\square) \cap \rho^j(\square)$ is a common edge if $i = j - 1$ and the origin otherwise.

Lemma 1 allows $\rho$ to serve as reparameterization for constructing $C^s$ manifolds for any $s$.

In the next section, we verify that at least one construction exists when $n = 8$ and hence $\partial_2 \rho^{[2]}(0,0) = \tau := 2\cos\frac{2\pi}{8} = \sqrt{2}$. We will use different numbers of segments $m$ for each edge, but the same number for opposing edges. Again with symbolic substitution, the following lemma is also straightforward to check.

*Lemma 2:* For $n \in \{4,6,8,10,12\}$, the $n$-fold composition $\rho^n$ with $\sigma_k := \tau\frac{m(k)-2}{m(k)}$ is the identity if $m(k) = m(k+n/2)$.
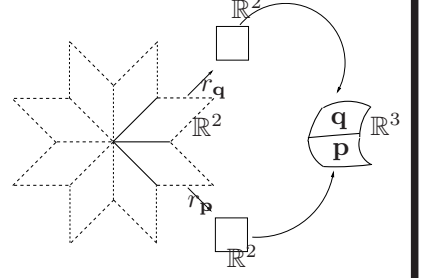
4

Alternatively, we can factor $\rho = r_{\mathbf{p}} \circ r_{\mathbf{q}}^{-1}$ into

$$r_{\mathbf{p}}(u,v) := \frac{1}{s + \eta v}\begin{bmatrix} -v \\ su + cv \end{bmatrix}, \qquad r_{\mathbf{q}}(u,v) := \frac{1}{s - \eta v}\begin{bmatrix} su - cv \\ v \end{bmatrix}, \quad (25)$$

where $\eta \in \mathbb{R}$, $\alpha := \frac{2\pi}{n}$, $c := \cos\alpha$, $s := \sin\alpha$ and arrive at

$$\partial^i(\mathbf{p} \circ r_{\mathbf{p}})(t,0) = \partial^i(\mathbf{q} \circ r_{\mathbf{q}})(t,0), \quad i = 0,\ldots,s. \qquad (2')$$

So, while $\rho$ gives a common domain across an edge, $n$ maps of type $r_{\mathbf{p}}$ yield a common preimage or chart to the patches of a vertex neighborhood.



## 4. CONSTRUCTIVE USE OF THE RATIONAL LINEAR TRANSITION MAP

To practically verify that the form of $\rho$ given in Theorem 1 is not only necessary but also sufficient for the generation of $C^s$ surfaces without shape defects, we sketch two such constructions, for $s = 1, 2$. We note that below we are not trying to create a general purpose high-end surfacing algorithm: such algorithms have to cope with design-induced distributions of irregular vertices of any valence. We only want to verify that the class of constructions using $\rho$ includes at least one reasonable member.

Still, the challenge is nontrivial. [PF09, Lemma 4] rules out general $C^1$ constructions with $\alpha$ linear everywhere; and (21) of the proof of Theorem 1 implies that $\alpha(t) := \partial_2\rho^{[2]}(t,0) = \tau(1-t) + \sigma t$ is necessarily linear everywhere. Moreover, the proof of [PF09, Lemma 4] is based on the existence of 4-valent vertices with tangents in X configuration, i.e. alternatingly collinear tangents $\tau_k = \tau_{k+2}$, $k = 1, 2$; and such 4-valent vertices naturally appear due to layout symmetry in all loops of the figure-8 shape Figure 1, *left*.

Fortunately, our setup falls into the one category identified as exceptional in the conclusion of [PF09] in that it allows linear $\alpha$ everywhere. We group the quadrilaterals into rectangular grids whose corner vertices are 8-valent and whose 8-valent vertices are connected by a chain of $m-1$, $m > 1$ vertices of valence 4. That is, for a given 8-valent point, the $k$th curve emanating from it has $m := m(k)$ pieces. For example, Figure 1, *left*, shows four such rectangular grids where, due to the low genus, each uses each 8-valent vertex twice.

With each rectangular grid we associate one tensor-product spline patch with uniform knots in the interior and full multiplicity of knots along the boundary so that the relevant coefficients are those of the Bernstein-Bézier form (*BB-form*; see (27) below). We partition $\alpha$ in (21) uniformly and set

$$\tau = \sqrt{2}, \; \sigma_k := \alpha_1^k, \quad \text{where } \alpha_\mu^k := \tau\frac{m(k) - 2\mu}{m(k)}, \quad \text{for } \mu = 0,\ldots,m. \qquad (26)$$

When $m(k) = m(k+4)$ then $\sigma_k = \sigma_{k+4}$ and Lemma 2 applies.

We denote the polynomial piece with index $\mu, \nu$ in the rectangular grid of the $k$th spline, $k = 1 \ldots n^0$, by $\mathbf{b}^{k,\mu,\nu}$. With $d = 2s + 1$ the bi-degree and $i, j$ enumerating the coefficients of one patch, the Bernstein Bézier form (BB) of one piece then has the form

$$\mathbf{b}^{k,\mu,\nu}(u,v) := \sum_{i=0}^{d}\sum_{j=0}^{d} b_{ij}^{k,\mu,\nu}\binom{d}{i}u^i(1-u)^{d-i}\binom{d}{j}v^j(1-v)^{d-j}. \qquad (27)$$

As usual in multi-variate constructions, the available degrees of freedom do not exactly match the number of constraints. Since our aim is to just show existence of a reasonable construction, our strategy for setting the default location of free variables can be simple: we interpret the vertices of the input quad mesh as spline coefficients with single knots and we ensure a $G^s$ transition between the spline pieces by least perturbation of the BB-coefficients along the spline boundaries. Due to the linear averaging of tangent configurations, the strategy is visible as in the V-shape in the perimeter of the central patch (see e.g. Figure 5, *right*). While the shorter formulas for the $G^1$ construction suffice for direct implementation, the $G^2$ construction is only explained at a high level.
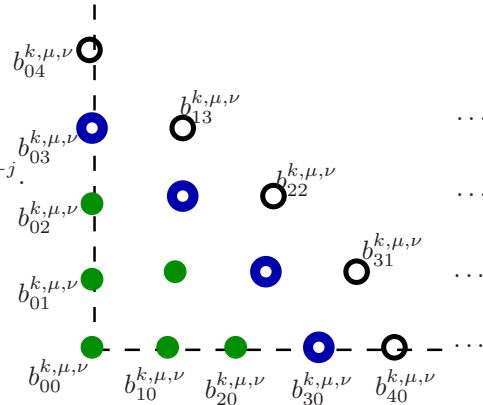


Fig. 3. Corner of the polynomial piece with index $\mu, \nu$ in the rectangular grid of the $k$th spline, $k = 1,\ldots,8$. We focus on $(\mu,\nu) = (0,0)$, the corner BB-patches of the spline, where the 8 patches meet and propagate the $G^s$ constraints along boundaries $\mu,\nu = \mu, 0$. The subscripts identify the BB-coefficients: for example, $b_{00}^{k,00}$ corresponds to the point shared by the splines which together with $b_{10}^{k,00}$ and $b_{01}^{k,00}$ defines the tangent plane.

### 4.1 $G^1$ construction

We choose $d = 3$. The unbiased $G^1$ constraints is

$$(\partial_2 \mathbf{q})(t,0) + (\partial_1 \mathbf{p})(0,t) = \alpha(t)\ (\partial_2 \mathbf{p})(0,t). \tag{28}$$

We note that linearity of $\alpha(t) := \tau(1-t) + \sigma t$ also has an upside since this is required ([PF09, Lemma 5]) for a bi-3 surface construction to cope well with higher-order saddles. Abbreviating, the $j$th set of coefficients of the $\mu$th segment of the $k$th edge,

$$u_j^{k,\mu} := b_{j+10}^{k,\mu 0} - b_{j0}^{k,\mu 0}, \quad v_j^{k,\mu} := b_{j1}^{k,\mu 0} - b_{j0}^{k,\mu 0}, \quad w_j^{k,\mu} := b_{1j}^{k-1,\mu 0} - b_{j0}^{k,\mu 0},$$

relation (28), split among $m$ segments along the boundary curve, yields for $\mu = 0, \ldots, m-1$, $\alpha_\mu^k := \tau \frac{m-2\mu}{m}$:

$$\delta_0^{k,\mu} = \alpha_\mu^k u_0^{k,\mu} \tag{29}$$

$$3\delta_1^{k,\mu} = 2\alpha_\mu^k u_1^{k,\mu} + \alpha_{\mu+1}^k u_0^{k,\mu} \tag{30}$$

$$3\delta_2^{k,\mu} = \alpha_\mu^k u_2^{k,\mu} + 2\alpha_{\mu+1}^k u_1^{k,\mu} \tag{31}$$

$$\delta_3^{k,\mu} = \alpha_{\mu+1}^k u_2^{k,\mu}, \tag{32}$$

where $\delta_j^{k,\mu} := v_j^{k,\mu} + w_j^{k,\mu}$. Nominally, these are $4m$ equations but, by enforcing continuity between the pieces, $(32)_{\mu=i} = (29)_{\mu=i+1}$, i.e. constraint (32) when substituting $\mu = i$ is identical to constraint (29) for $\mu = i+1$ so that there are only $3m$ constraints to check.

### 8-valent vertex neighborhood

We initialize the BB-coefficients $\mathbf{x}_{ij} := b_{ij}^{k,00}$ for $i + j < 3$ by approximating the limit of the Catmull-Clark surface. That is, we surround a vertex $p^0$ of valence 8 (Fig. 4) by 8 patches in BB-form (to form the corner pieces of a spline). We set $\mathbf{x}_{00}$ to the limit of $p^0$ under Catmull-Clark subdivision (red circle in Fig. 4 *middle*) and place the $\mathbf{x}_{10}^k$ for $k = 1 \ldots 8$ (blue circles in Fig. 4 *middle*) into a common plane spanned by $\mathbf{x}_{00}$ and the real and the imaginary part of the vector of complex numbers obtained for valence 8 and angle $\frac{2\pi}{8} = \frac{\pi}{4}$:

$$\mathbf{t}^* := \frac{4}{3\kappa(\kappa-2)} \sum_{j=1}^{8} \left((\kappa-4)e^{\frac{\sqrt{-1}\pi}{4}(j-1)}p^{2j-1} + (e^{\frac{\sqrt{-1}\pi}{4}(j-1)} + e^{\frac{\sqrt{-1}\pi}{4}j})p^{2j}\right), \quad e = \exp, \tag{33}$$



$$\mathbf{x}_{00} = \mathbf{x}_{00}^k := \frac{1}{104} \sum_{j=1}^{8} 8p^0 + 4p^{2j-1} + p^{2j}, \tag{34}$$

$$\mathbf{x}_{10}^k := \mathbf{x}_{00}^k + \text{Re}(\mathbf{t}^*)\cos\frac{\pi k}{4} + \text{Im}(\mathbf{t}^*)\sin\frac{\pi k}{4}, \tag{35}$$

$$\mathbf{x}_{11}^k := \frac{1}{9}(4p^0 + 2(p^{2k+1} + p^{2k+3}) + p^{2k+2}). \tag{36}$$

For $\tau = \sqrt{2}$, $\kappa := \frac{1}{\tau} + 5 + \sqrt{(\frac{1}{\tau} + 9)(\frac{1}{\tau} + 1)}$, the common plane is the Catmull-Clark tangent plane. Figure 5, *middle*, shows the BB-patches after initialization.
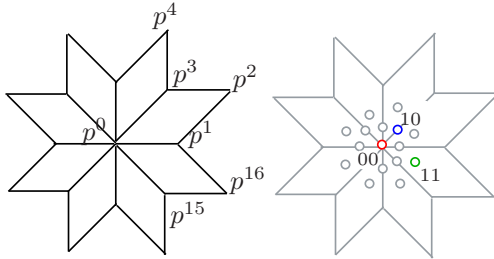
Fig. 4. *left*: extraordinary vertex $p^0$ with 8 direct neighbors $p^{2k-1}$, $k = 1 \ldots 8$. *right*: limit point $\mathbf{x}_{00}$, tangent points $\mathbf{x}_{10}^k$ and 'twist' coefficients $\mathbf{x}_{11}^k$.

*Propagation of the $G^1$ correction* along spline boundaries. Let $\bar{b}_{20}^{k,00}$ and $\bar{b}_{30}^{k,00}$ be the BB-coefficients derived from interpreting the vertices of the quad-mesh as bi-3 spline coefficients. We adjust $b_{20}^{k,00}$ and $b_{30}^{k,00}$ to enforce (30) for the first BB-piece of the spline (and symmetrically at the other 8-valent vertex), setting

$$b_{20}^{k,00} := b_{10}^{k,00} + u_1^{k,0}, \quad u_1^{k,0} := \frac{3(v_1^{k,0} + w_1^{k,0}) - \alpha_1^k u_0^{k,0}}{2\alpha_0^k}, \tag{37}$$

$$b_{21}^{k,00} := \bar{b}_{21}^{k,00} + \delta_0, \quad \delta_0 := \bar{b}_{20}^{k,00} - b_{20}^{k,00} \tag{38}$$

$$b_{30}^{k,00} := \frac{b_{20}^{k,00} + b_{10}^{k,10}}{2}, \quad \delta_1 := \bar{b}_{30}^{k,00} - b_{30}^{k,00}, \tag{39}$$

$$b_{31}^{k,00} := \tilde{b}_{31}^{k,00} + \delta_1 \tag{40}$$

and propagate the adjustment by modifying

$$v_j^{k,\mu} \leftarrow v_j^{k,\mu} + \delta_j^{k,\mu}/2, \quad w_j^{k,\mu} \leftarrow w_j^{k,\mu} + \delta_j^{k,\mu}/2, \tag{41}$$

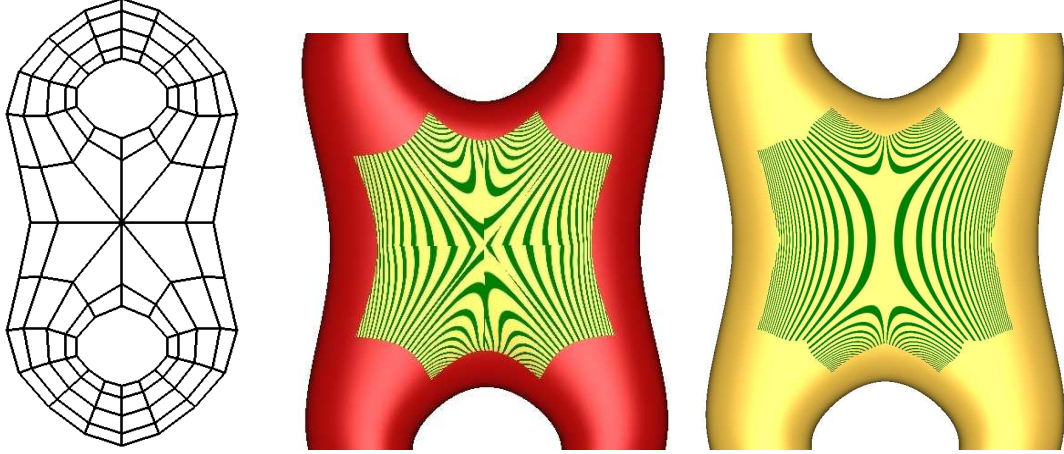for $j = 1, 2, 3$ and $\mu = 1, \ldots, m-1$ to satisfy $(29)_{\mu,k}$, $(30)_{\mu,k}$, $(31)_{\mu,k}$.

Fig. 5. $G^1$ construction. (*left*) The BB-control-net with the number of segments is chosen as $m = 5, 12, 5, 12, 5, 12, 5, 12$. (*middle*) $C^0$-connected patches (note the slight discontinuities in the highlight lines) in BB-form after initialization. (The red surface stems from the unperturbed quad mesh interpreted as control net of a tensor-product spline of degree bi-3.) (*right*) Smooth surface. With the control net away from the boundaries unchanged, the linear averaging of the valence 8-configurations cause an initial V-shaped frontier (but not dip) in the patch propagation through the loops.

## 4.2 $G^2$ construction

The splines of our $G^2$ construction are of degree bi-5. As in the $G^1$ case, we inherit the basic shape from the quad mesh by interpreting the mesh vertices as spline control points. We can therefore focus on the outermost three boundary layers in BB-form, i.e. coefficients where at least one index is less or equal to 2. We need to enforce

$$(\partial_2^2 \mathbf{q})(t, 0) = (\partial_1^2 \mathbf{p})(0, t) - 2\alpha(t)(\partial_1 \partial_2 \mathbf{p})(0, t) + \alpha^2(t)(\partial_2^2 \mathbf{p})(0, t) \qquad (13')$$
$$- 2(\tau - \sigma)\alpha(t)(\partial_2 \mathbf{p})(0, t) + 2(\tau - \sigma)(\partial_1 \mathbf{p})(0, t).$$

*8-valent vertex neighborhood*

As in the $G^1$ case, we need to first determine the total degree $2s$-jet at the vertices, i.e. the BB-control-points with index summing to at most 4. These are the points in Figure 3. The points are treated in three groups. All solid, green points with index summing to at most 2, of all eight patches have no more than 6 degrees of freedom total, since that defines the local $C^2$ expansion. As a reasonable heuristic, we borrow the expansions of the $G^1$ construction, degree-raised to 5: For each patch, we trace a $C^2$ expansion around the 8-valent vertex and then average the $C^2$ expansions. The key challenge (see [HPS10]) is to solve, for fixed boundary coefficients with index 30 which agree with those with index 03 of the preceding patch, for the 16 coefficients with subscript 12 and 21 (blue, solid circle layer). For this, we substitute the $G^1$ constraints involving $b_{12}^{k-1,00}$ and $b_{21}^{k,00}$ into the $G^2$ constraints in the same coefficients and eliminate the coefficients with subscript 21. This yields a $8 \times 8$ system of constraints in terms of the 8-vector $\mathbf{x}_{12}$ whose $k$th entry is $\mathbf{x}_{12}^k := b_{12}^{k,00}$.

$$\mathbf{M}\mathbf{x}_{12} = \mathbf{r}, \qquad \mathbf{M}_{kj} := \begin{cases} \frac{\tau}{2}, & |k - j| = 1 \\ 2, & k = j \\ 0, & else. \end{cases}, \qquad (42)$$
$$\mathbf{r}_k := (2\tau - \sigma)\mathbf{x}_{11}^k + 2\mathbf{x}_{30}^k + (2\tau\sigma - 4)\mathbf{x}_{20}^k - 2\mathbf{x}_{11}^{k-1} + \tau\mathbf{x}_{30}^{k-1}.$$

The matrix $\mathbf{M}$ is invertible and we get a unique solution for the coefficients with subscripts 12 and, by back substitution into the $G^1$ constraint, for those with subscript 21. Finally, with the coefficients with subscript 22 taken from the spline surface, we can solve the $G^1$ and the $G^2$ constraints involving $b_{13}^{k-1,00}$ and $b_{31}^{k,00}$ uniquely in those variables.

*Propagation of the $G^2$ correction* along spline boundaries. As in the $G^1$ case, we propagate a perturbation of the initialization along the boundary to obtain a $G^2$ transition between the spline patches, leaving the second layer of coefficients $b_{j2}^{k,\mu0}$ unchanged.

Figure 5 shows that the simple construction without otpimization yields reasonable results.

## 5. CONCLUSION

Theorem 1 shows the uniqueness of the lowest-degree, namely rational linear (projectively linear) bi-variate reparameterization for constructing at least $C^2$-smooth surfaces with unbiased geometric continuity constraints.
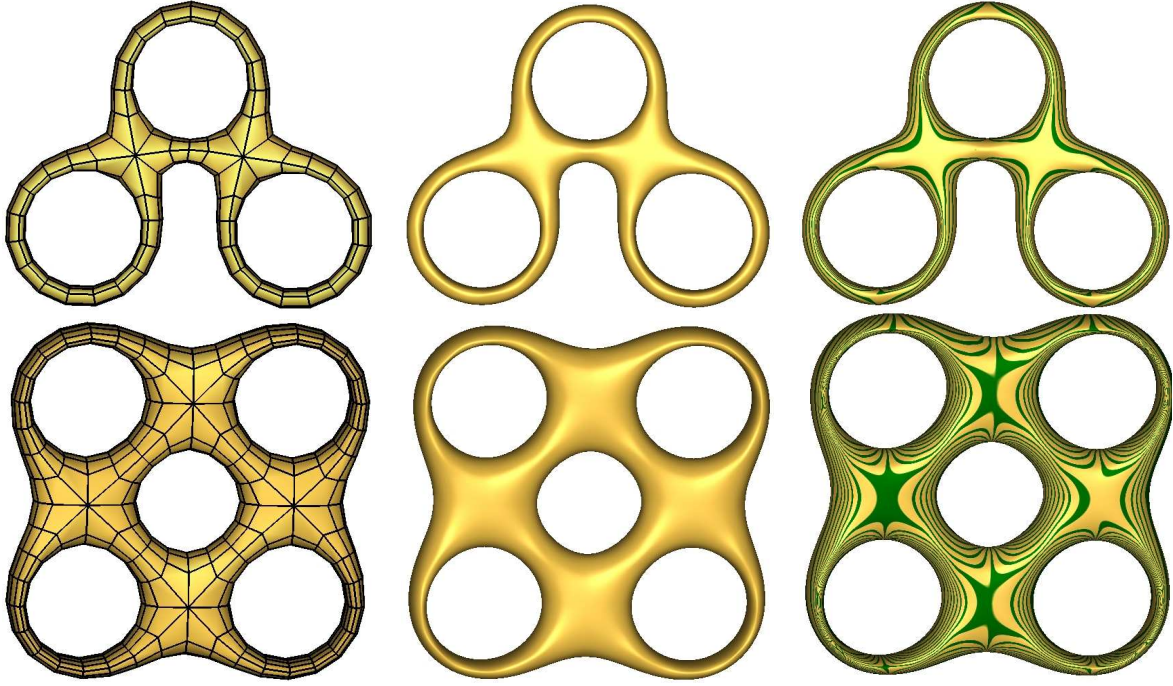
Fig. 6.   *top* Genus 3 surface with four vertices of valence 8. *bottom* genus 5 surface with eight vertices of valence 8.
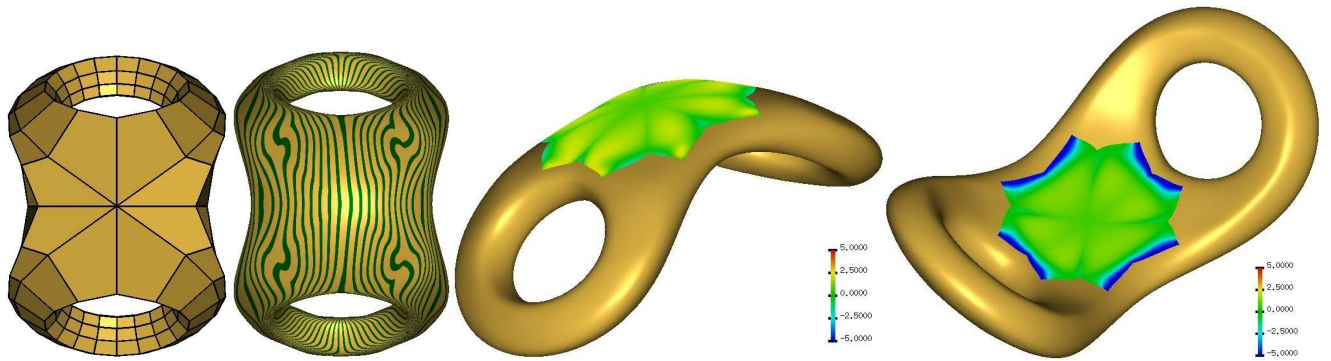


Fig. 7.   Bent figure-8: layout, reflection lines, (non-negative) Gauss curvature.

Lemma 1 and 2 show that the rational linear reparameterization is admissible with $C^s$ constructions for any $s$. *It is the simplest such map.*

Conversely, two concrete constructions outlined in Section 4, verify the sufficiency of the reparameterization for generating smooth manifolds of any non-zero genus (Figure 7) and without necessary shape problems, for quad-meshes with isolated vertices of valence 8. Figure 1 shows a saddle and Figure 7 a convex neighborhood of the 8-valent point.

We emphasize that the algorithms reprsent a proof of concept and we do not advocate the algorithms as general-purpose, high-end surface constructions. In high-end surface constructions, *local shape considerations* rather than the overall genus are the main reason for introducing vertices of arbitrary valence. Also for better shape one can choose the polynomial degree of the splines for a $C^s$ surface to be higher than $2s + 1$.

The low degree surface parameterizations with simplest transition functions are expected to find use as computational domains, analogous, but simpler than, existing construction such as spline orbifolds [WP98].

Triangulations analogous to our quad meshes are regular, i.e. the vertices are 6-valent, everywhere except for $-\chi$ isolated vertices of valence 12. The theorem and the two lemmas of Section 3 apply unchanged to such triangulations, with $\tau := \sqrt{3}$. The characterization of admissible rational linear reparameterizations also applies to genus 0. Here $n = 3$ and $\tau := -1$; $\sigma_1 = \sigma_2 = \sigma_3$ must hold in order that $\rho_3 \circ \rho_2 \circ \rho_1 = \text{id}$.

## REFERENCES

[GHJ⁺08] Xianfeng Gu, Ying He, Miao Jin, Feng Luo, Hong Qin, and Shing-Tung Yau. Manifold splines with a single extraordinary point. *Computer-Aided Design*, 40(6):676–690, 2008.

[Hah89] Jorg M. Hahn. Geometric continuous patch complexes. *Computer Aided Geometric Design*, 6(1):55–67, 1989.

[HPS10] Tamas Hermann, Jorg Peters, and Tim Strotman. Constraints on curve networks suitable for $G^2$ interpolation. Technical Report REP-2010-490, Dept of CISE, University of Florida.

[KP09] K. Karčiauskas and J. Peters. Assembling curvature continuous surfaces from triangular patches. *SMI 26/105, Computers and Graphics*, 2009.

[LS08] Charles T. Loop and Scott Schaefer. $G^2$ tensor product splines over extraordinary vertices. *Comput. Graph. Forum*, 27(5):1373–1382, 2008.

[Mil58] J. W. Milnor. On the existence of a connection with curvature zero. *Comm. Math. Helv.*, 32(1):215223, 1958.

[Pet02] J. Peters. Geometric continuity. In *Handbook of Computer Aided Geometric Design*, pages 193–229. Elsevier, 2002.

[PF09] J. Peters and Jianhua Fan. On the complexity of smooth spline surfaces from quad meshes. *Computer-Aided Geometric Design*, 27:96–105, 2009.

[wik09] wiki. Uniformization theorem, 2009. http://en.wikipedia.org/wiki/Uniformization_theorem.

[WP98] Johannes Wallner and Helmut Pottmann. Spline orbifolds. In A. Le Méhauté, C. Rabut, and L. L. Schumaker, editors, *Curves and Surfaces with Applications in CAGD*, pages 445–464, 1998.

[YZ04] Lexing Ying and Denis Zorin. A simple manifold-based construction of surfaces of arbitrary smoothness. *ACM Transactions on Graphics*, 23(3):271–275, August 2004.